EmAIT

EMERGING ADVANCES IN INTEGRATED TECHNOLOGY
e-ISSN: 2773-5540

Vol. 7 No. 1 (2026) 23-32
https://publisher.uthm.edu.my/ojs/index.php/emait

Z-Scanning Analysis of Non-Linear Optical Properties of Biodiesel Prepared Via Transesterification Reaction

Siti Noraiza Ab Razak[1]*, Mohamad Aizat Abu Bakar[2], Nurul Nadia Adnan[3], Muhammad Sufi Roslan[1], Mundzir Abdullah[4], Ganesan Krishnan[5], Nik Noor Haryatul Eleena Nik Mahmud[3]

[1] *Department of Science and Mathematics, Centre for Diploma Studies, Universiti Tun Hussein Onn Malaysia, 84600 Muar, Johor, MALAYSIA*

[2] *Malaysian Meteorological Department, Ministry of Natural Resources, Environment & Climate Change, 46667 Petaling Jaya, Selangor, MALAYSIA*

[3] *Faculty of Applied Sciences and Technology, Universiti Tun Hussein Onn Malaysia, 84600 Muar Johor, MALAYSIA*

[4] *Institute of Nano Optoelectronics Research and Technology (INOR), Universiti Sains Malaysia, 11800 Penang, MALAYSIA*

[5] *Laser Centre, Institute Ibnu Sina for Scientific and Industrial Research (IS-SIR), Universiti Teknologi Malaysia, 81310 Skudai, Johor, MALAYSIA*

*Corresponding Author: noraiza@uthm.edu.my
DOI: https://doi.org/10.30880/emait.2026.07.01.003

Article Info

Received: 1 April 2026
Accepted: 23 June 2026
Available online: 30 June 2026

Keywords

Waste cooking oil, nonlinear absorption, transesterification, one-step transesterification, Levenberg-Marquadt algorithm

Abstract

This paper explores the nonlinear optical properties (NLO) of biodiesel (BD) produced from waste cooking oil (WCO), a sustainable and environmentally friendly alternative to conventional diesel fuel, using the Z-scan method. The study investigates the optical, chemical, and physical characteristics of BD derived from WCO through transesterification. Both the physical and chemical properties, as well as the NLO, were characterized. The physical and chemical properties and nonlinear optical properties were characterized. The density of BD is 0.85 gcm^{-3} and kinematic viscosity is 5.76 mm^2s^{-1}. The Fourier Transform Infrared (FTIR) spectrum results show methyl ester is presented in BD converted from WCO. The experimental results, obtained using the Z-scan method, revealed that the nonlinear optical properties n_2, β and χ^3 are 1.76×10^{-14} cm^2/W, 7.80×10^{-4} cm/W and 1.046×10^{-5}, respectively. These findings suggest that BD exhibits potential applications in optical switching, laser technology, signal processing, optical limiting, and optoelectronic devices.

1. Introduction

Nowadays, numerous research works are actively exploring nonlinear optical (NLO) properties of various materials, motivated by promising applications in optical switching [1], laser technology [2], signal processing [3], optical limiting [4], and optoelectronic devices [5]. The phenomena in NLO arise from intricate interactions between materials and intense light, with two primary mechanisms at play: electronic and non-electronic processes [6]. Non-electronic processes occur without involving electronic transitions within the material when subjected to intense light, whereas electronic processes involve the intricate interactions between the active electrons within a material and intense light [7].

NLO may be investigated using a variety of methods, including beam distortion studies [8], Z-scan method [9], degenerate four-wave mixing [10, 11], nonlinear interferometry [12], three-wave frequency mixing [13], and others. In comparison to the Z-scan method, these approaches need a more sophisticated experimental setup, especially since beam distortions lack sensitivity without precise wave propagation analyses. Owing to its very efficient, precise, and simple optical way of obtaining both the nonlinear refractive index and the nonlinear absorption coefficient (NLA), the Z-scan method has therefore been widely used in material characterization [14]. Z-scan methods with both closed aperture (CA) and open aperture (OA) are frequently used to calculate a material's nonlinear refractive index (NLR) and nonlinear absorption (NLA) [15]. The attainment of high stabile nonlinearity and exceptional optical properties stands as the primary prerequisites for the efficacy of an optical nonlinear material [16]. Furthermore, this technique exhibits a distinctive ability to provide an extremely sensitive singular measurement for both the NLA and NLR concurrently, employing a solitary beam. Numerous materials, including organic dyes [18], metal halides [19,20], and 2D materials [21], have been studied extensively due to their documented nonlinear optical characteristics. Across the globe, biodiesel (BD) fuels are gaining momentum as a viable alternative to diesel fuel in automotive engines or as an ingredient in blending [22].

The advantages of BD encompass decreased greenhouse gas emissions, social stability, regional development, energy security and energy independence [23]. In the pursuit of a sustainable and eco-friendly future, thorough exploration of alternative energy sources is imperative. BD, originating from organic materials, has become a notable renewable fuel candidate. Waste cooking oil (WCO), an exceptional and easily accessible resource, presents significant potential for BD production [24]. Employing WCO as a raw material for BD synthesis presents several environmental advantages. Firstly, it helps reduce the disposal of WCO into landfills or water bodies, preventing pollution and potential health hazards. BD from WCO is readily biodegradable, whereas commercial diesel is persistent and takes longer to break down in the environment. This characteristic of BD reduces the environmental impact in case of spills or leaks. Second, when compared to fossil fuels, the manufacture of BD from WCO produces much lower amounts of greenhouse gases, contributing to a reduction in carbon dioxide (CO2) and other harmful emissions. This technique also contributes to the reduction of depletion of fossil fuel reserves, encouraging long-term sustainability [25, 26].

To the best of our knowledge, there is no existing literature that has provided data on nonlinear optical properties of BD synthesis. Therefore, this research paper explores the NLO characteristics of BD orchestrated from palm WCO by employing Z-scan analysis. Additionally, this study examines the optical, chemical, and physical characteristics of BD produced through the transesterification process of WCO. Furthermore, this research paper will conduct a comprehensive analysis of the chemical and physical properties of BD by comparing it with commercially available BD in the market. Transesterification is the process that synthesizes BD from WCO by converting the triglycerides in the oil into methyl or ethyl esters, which are the main components of BD. The process necessitates adding alcohol, usually methanol or ethanol, and a catalyst such as sodium hydroxide (NaOH) or potassium hydroxide (KOH) [27]. Due to its simplicity and compatibility with conventional equipment, the transesterification process is a viable option for large-scale production. There are notable economic advantages to synthesizing BD from WCO. WCO is commonly available and can be obtained at minimal or no expense from food establishments like restaurants and fast-food chains. This easy access to WCO cuts down on production costs, making BD a cheaper alternative to regular diesel fuel. Moreover, the local production and use of biodiesel promote energy independence, lessen the need for imported fossil fuels, and generate economic opportunities for local areas [28, 29]. The utilization of WCO for BD synthesis holds significant potential, however, challenges related to the variability in quality and composition of the WCO can negatively impact the process efficiency and the stability of the final product. Effective pre-treatment methods, including filtration and purification, are essential for the removal of impurities and contaminants, thereby ensuring a cleaner and more consistent final product. Additionally, the procurement and logistical management of WCO could present formidable challenges, necessitate the implementation of effective collection mechanisms and foster partnerships with local enterprises.

Additionally, the choice of catalyst utilized in the transesterification process holds significant sway in the production of environmentally sustainable BD. Homogeneous and heterogeneous catalysts are commonly employed in industrial settings. Numerous researchers have opted to substitute detrimental catalysts with naturally sourced alternatives, such as eggshells, seashells [30], ripe and unripe plantain peels [31], dolomite [32], and various others. Despite these alternatives, the choice of catalyst appears to have minimal impact on the produced BD, as its primary function during transesterification is to accelerate the synthesis process. Consequently, owing to its strong alkali characteristic, this research employed NaOH as the catalyst.

2. Methodology

The methodology consists of two main parts; (1) synthesis of WCO into BD and (2) chemical and physical properties of BD.

2.1 Synthesis of Biodiesel

The overall procedure of one-step transesterification for synthesizing WCO into BD involves three main steps: pre-treatment of WCO, transesterification, and a filtering process for the crude BD. Initially, the WCO was placed in a container for 24 hours, facilitating the settling of larger particles to the bottom. This step aimed at preparing the WCO for subsequent filtration. Following this, the WCO underwent filtration using filter paper to remove smaller suspended impurities. The filtered WCO was then heated to 110°C while continuously stirred for 30 minutes to evaporate any remaining water. Finally, the treated WCO was allowed to cool to room temperature. The treated WCO underwent a one-step transesterification process where a catalyst; a solution containing 12 g of NaOH and 150 ml of methyl alcohol; was added to the WCO. This mixture was thoroughly stirred at a temperature of 55°C. After 2 hours, the sample was filtered to eliminate suspended glycerine. Following that, the sample was washed using distilled water to remove dissolved glycerine. The washed BD was left for 24 hours to allow the glycerine to sediment at the bottom. It took five more repetitions of the method to produce clear and pure biodiesel [1]. The BD was put in a sealed container to protect it from outside contaminants. Fig. 1 (a) shows the untreated WCO, while Fig. 1 (b) shows the BD as an outcome from the transesterification process.

(a) (b)

Fig. 1 *One-step transesterification process of WCO into BD*

2.2 Z-Scanning of Biodiesel

By integrating OA and CA into a single setup, the Z-scan method lets us collect the transmitted light signal from the BD sample simultaneously, as depicted in Fig. 2. In this setup, a diode laser serves as the high-intensity light source, emitting light at a wavelength of 637 nm in continuous wave (CW) mode. A plano-convex lens with a 25 cm focal length is utilized to reshape the beam diameter as it propagates along the scanning area. A motorized linear translation stage is positioned under the laser beam path with a customized sample holder set to move the sample at a distance of 300 mm and a velocity of 30 mm/s. The transmitted laser beam was split into two by using the quartz beam splitter cube with a 50:50 reflectance to transmittance ratio. The first photon signal is directed towards the photodiode, which is coupled with a focusing lens. The lens gathers the entire incoming light signal, designated as the OA measurement. The second light signal that passes through the beam splitter undergoes partial blocking, enables only fractions of the incoming light signal to reach the photodiode. This configuration is referred to as the CA measurement [33]. Both apertures are fitted with the neutral density filter to reduce the laser beam intensity accordingly to avoid potential damage to the photodiode sensor. NLO properties of BD are quantified from the fitting process with data obtained from scanning according to the Levenberg-Marquadt algorithm. To obtain the nonlinear absorption coefficient β, the fitting was done on the transmittance data points obtained from the OA arm. The OA transmittance intensity along the z direction is normalized T(z) and fitted by using the Eq. 1 and Eq. 2 [33].

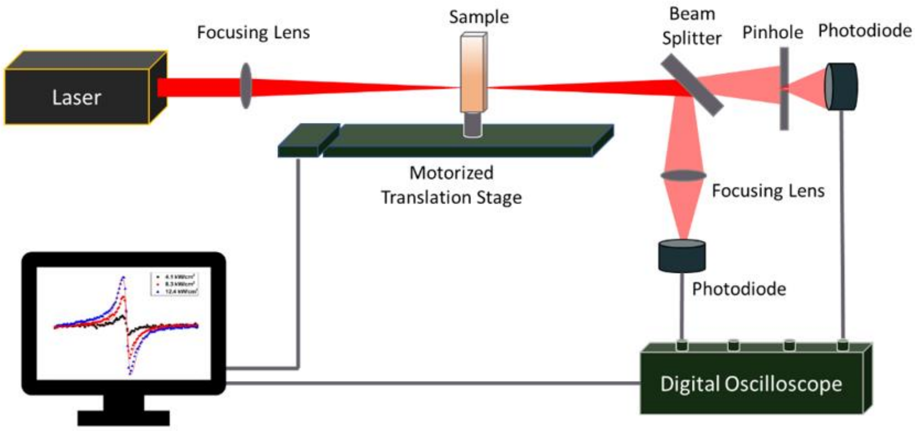

Fig. 2 *Schematic of Z-scan setup*

$$T(z, s = 1) = \sum_{m-0}^{\infty} \frac{[-q_0(z)]^m}{(m+1)^{3/2}} \tag{1}$$

with $q_0(z) < 1$, where

$$q_0(z) = \frac{\beta I_o L_{eff}}{\left(1 + \frac{z^2}{{z_R}^2}\right)} \tag{2}$$

The $z_R = \frac{k{\omega_o}^2}{2}$ is the Rayleigh range, ω_o is the Gaussian beam waist radius, I_o is the on-axis intensity at the focus $(z = 0)$, L_{eff} is the effective thickness of the sample and $k = \frac{2\pi}{\lambda}$ is the wave vector. Simultaneously, the oscilloscope captures CA data points to record the NLR response. It is worth noting the potential impact of using a CW mode laser on NLO properties. As it differs temporally from an ultrafast laser, the continuous deposition of photon energy on the target area leads to the accumulation of heat, which may affect the electronic structure. In conducting NLO measurements under the CW mode, the fitting process considers significant thermal effects [17,34]. Consequently, thermal lensing modelling (TLM) is employed to address such circumstances. The TLM equation used for fitting (Eq. 3), was derived from the SBF [35].

$$T(z) = \frac{1}{1 + \theta\left[\frac{2\left(\frac{z}{z_R}\right)}{1 + \left(\frac{z}{z_R}\right)^2}\right]} \tag{3}$$

where

$$\theta = \frac{2\pi L n_2 I_o}{\lambda \varepsilon_o c n_o} \tag{4}$$

The L is the thickness of the sample, λ is the wavelength used as the irradiation source, ε_o is the permittivity of free space, c is the speed of light in vacuum and n_o is the refractive index of sample at setup wavelength. The 3rd order nonlinear susceptibilities χ^3 is considered as a complex quantity which consists of real and imaginary parts.

$$|\chi^3| = \sqrt{(Re(\chi^3))^2 + (I_m(\chi^3))^2} \tag{5}$$

The obtained value of β and n_2 from fitting process are adopted for the calculation to determine the real and imaginary component of complex nonlinear susceptibilities equation shown in Eq. 6 and Eq. 7.

$$Re\ \chi^3(esu) = 10^{-4}\frac{\varepsilon_o c^2 {n_o}^2}{\pi^2} n^2 (cm^2/W) \tag{6}$$

$$I_m\ \chi^3\ (esu) = 10^{-2}\frac{\varepsilon_o c^2 {n_o}^2 \lambda}{4\pi^2} \beta\ (cm/W) \tag{7}$$

3. Result and Discussion

3.1 Density and Viscosity of Biodiesel

The density of BD synthesis from WCO has been calculated to be 0.85 gcm^{-3} using the standard method using a capillary relative density bottle of 50 ml in volume.

Table 1 *Density and kinematic viscosity comparison of biodiesel produced from different feedstocks* [36]

Feedstock	Density (gcm^{-3})	Kinematic Viscosity (mm^2s^{-1})
Sunflower oil	0.86	4.40
Soybean oil	0.89	4.02
Rapeseed oil	0.88	5.65
Palm oil	0.88	3.85
Linseed oil	0.89	4.01
Jatropha oil	0.89	5.15

Table 1 presents BD densities obtained from various feedstock such as sunflower oils, soybean, rapeseed, palm, linseed, and jatropha [36]. The results indicate that the density of BD derived from WCO falls within a similar range to BD produced from other feedstocks. This similarity is attributed to the presence of methyl ester in the BD converted from WCO. The kinematic viscosity of biodiesel produced from WCO was calculated to be 5.76 mm^2s^{-1}. The result shows that the kinematic viscosity of BD converted from WCO was the highest compared to another feedstock. The high value of kinematic viscosity was caused by the high fatty acid composition. When the concentration of fatty acids increases, the kinematic viscosity of BD also increases in value [37].

3.2 Non-linear Optical Properties of Biodiesel

The NLO responses are successfully observed in both apertures with a clear indication of NLO behaviour. The exposure of a high-intensity electric field to oil samples results in a unique transmitted signal which reveals the differences in their NLO properties. As the oil samples are displaced along the z-axis, from the near-field position, the laser irradiation intensity on the samples increases gradually and maxes out at the focal distance position. Subsequently, the intensity returns to the initial level as the sample is moved away to the far-field area at the end of the translation stage. The scanned sample produced a distinctive transmittance pattern which correlates to NLR and NLA responses according to the set-up of the photodiodes. The resulting light signals captured on the CA, however, incorporate information from both the NLR and NLA response. Consequently, the CA transmission value is divided over the value of OA transmission to eliminate the nonparametric influence on the measured n2 value [38].

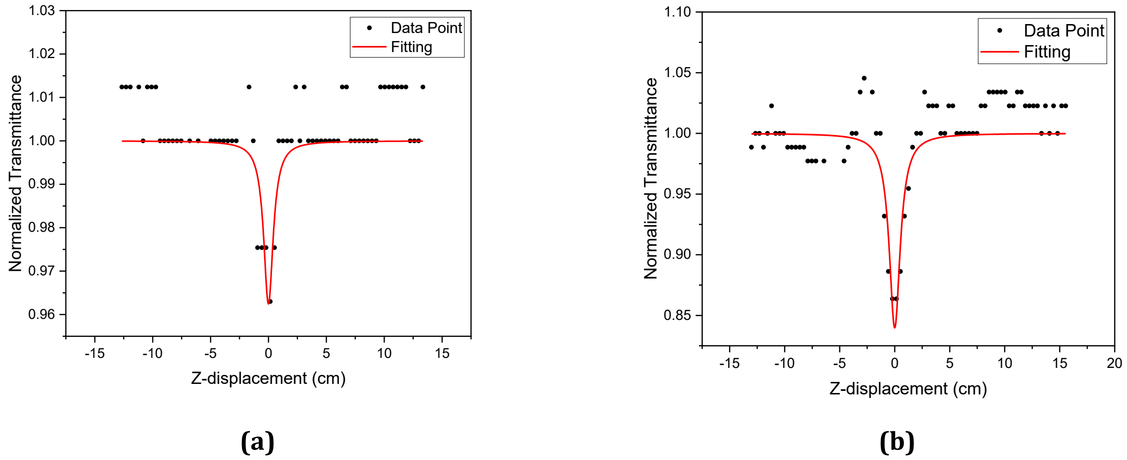

Fig. 3 *Open apertures result of oil sample (a) before; and (b) after transesterification process*

Fig. 3 shows the normalized results from OA for both samples exhibit a consistent pattern, indicating a substantial reduction in transmittance at the displacement position of 0 cm. In contrast, the transmittance levels remain stable for other positions. During sample translation, changes in the light signal transmission through the focusing lens occur, corresponding to variations in the beam area along the z-direction. All oil samples demonstrate a valley pattern along the z-direction, centered at the beam waist, signifying the occurrence of the RSA mechanism, i.e., positive β. The observed apparent RSA might be the contribution from the excited state absorption (ESA) from a specific excited state to higher excited states. Additionally, differences in photon energy and band gap energy, where $E_p < E_g$, suggest that the dominant mechanism is two-photon absorption. As the input intensity further increases, a non-resonant excitation occurs. This results in the absorption cross-section of the excited state surpassing that of the ground state. The excitation of an already excited state electron into an unoccupied state in the conduction band is known as intra-band absorption. Typically, in a transparent medium, a single photon does not have enough energy to excite electrons from the ground state. However, if the band gap energy is equivalent to the two or more photons energy, multi-photon photon absorption takes place. Both two-photon absorption and free carrier absorption are independent of the input light wavelength provided the photon energy remains below the material band gap. Additionally, thermal effects induced contribute to a self-scattering effect, potentially lower the transmitted signal.

Results from CA also produced similar trends of transmittance for both samples. As shown in Fig. 4 (a), in CA, the movement of the sample from near-field (-z displacement) to the focal point increases the electric field intensity exposed on the samples forcing an increase of photon absorption which in turn affects the material refractive index. The shifting of material refractivity affected the curvature of the Gaussian beam wavefront near the focus point. This causes a general increase in the far-field radiation divergence [39]. As the sample approaches the beam waist displacement (z=0), the beam divergence exacerbates manifesting in a gradual decrease of transmittance intensity. At the beam waist area, the samples exhibit a sharp dive in transmittance intensity followed by a sudden sharp rise close to the focal position on both the negative and positive sides. The sudden rise is contributed by the elongated curvature of the wavefront which significantly reduces the beam divergence causing a spike in intensity. However, further sample displacement towards the far-field position showed a gradual decrease of transmittance intensity until it reached the initial level. This results in the formation of a peak and valley around the beam waist which indicates the occurrence of NLR as observed in Fig. 4 (b).

Emerging Advances in Integrated Technology Vol. 7 No. 1 (2026) p. 23-32

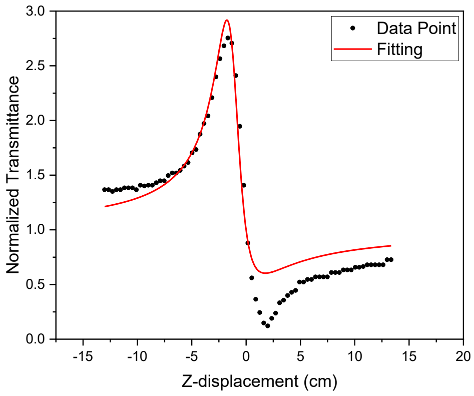

(a)

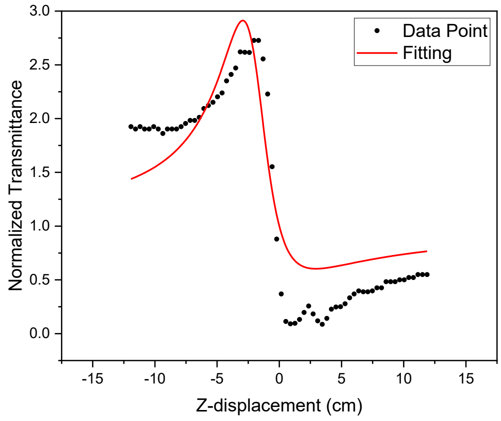

(b)

Fig. 4 *Closed apertures result of oil sample (a) before; and (b) after transesterification process*

For CW laser, thermalization induced by the laser may also cause slight random fluctuation of density thus contributing to NLR of the oil samples. The self-defocusing which fulfils the requirement for a trigger that is only under laser power exceeds the critical power threshold [40]. This phenomena of self-defocusing behavior which arise during irradiation can be described through several mechanisms but in this experimental setup, it is mainly due to the thermal lensing effect. The CW laser supplies photon continuous duration well over the exciton decay time, τ value of any sample where it reaches a steady state of heat exchange on the irradiated zone forming a temporary thermal lens inside the sample. This phenomenon is characterized as a thermal nonlinear optical effect, wherein the absorption of light energy on the irradiance area induces a change in the internal refractive index, leading to the diffusion of a spatial temperature profile [6]. The data acquired from the oscilloscope undergoes further processing for quantitative analysis. To determine the magnitude of n2, the CA transmittance profile along the z direction is normalized T(z) and calculated using the thermal lensing model based on the modified Sheik-Bahae z-scan theory [41]. The transmittance value of CA is then divided by the OA transmission value to mitigate nonparametric influences on the true n2 value.

Table 2 *Nonlinear optical properties of WCO and BD*

Parameter	WCO	BD
$n_2(cm^2/W)$	1.74 x10^{-14}	1.76 x10^{-14}
$\mathrm{Re}\,\chi^{(3)}(esu)$	1.44 x10^{-13}	1.49 x10^{-13}
$\beta(cm/W)$	4.1 x10^{-3}	7.80 x10^{-4}
$\mathrm{Im}\,\chi^{(3)}(esu)$	5.50 x10^{-5}	1.05 x10^{-5}
χ^3	5.50 x10^{-5}	1.046 x10^{-5}

Table 2 illustrates the nonlinear optical properties of WCO and BD. The calculated n_2 value is higher for the BD sample at 1.76 x10^{-14} cm^2/W while untreated WCO only at 1.74 x10^{-14} cm^2/W which correlates with the higher viscosity and density compared to the untreated WCO. However, the β shows a significant difference of a magnitude at 41x10^{-4} cm/W and 7.80 x10^{-4} cm/W for WCO and BD samples, respectively. This is caused by the presence of impurities in untreated WCO which provide a larger interactable surface area for greater light absorption compared to the purer oil sample of biodiesel. The range of the χ^3 for the samples is well within the expected range of 10^{-5} compared to other finding [42]. This cemented the potential for the BD to be used as a nonlinear optical material, especially for application in high-temperature and hydrophobic conditions.

4. Conclusion

In conclusion, BD synthesis from WCO represents a sustainable solution with a multitude of environmental and economic benefits. This research has successfully employed Z-scan method to validate the nonlinear optical properties of BD achieved through transesterification. The results reveal significant values for BD's nonlinear optical properties with n_2, β, and χ^3 measured at 1.76×10^{-14} cm^2/W, 7.80×10^{-4} cm/W and 1.046×10^{-5}, respectively.

These findings suggest the potential applications of BD in diverse fields such as optical switching, laser technology, signal processing, optical limiting, and optoelectronic devices.

Acknowledgement

This research was supported by Universiti Tun Hussein Onn Malaysia (UTHM) through Tier 1 (vot Q438). The authors would like to thank Universiti Sains Malaysia and Universiti Teknologi Malaysia for their facilities and services during this research.

Conflict of Interest

Authors declare that there is no conflict of interests regarding the publication of the paper.

Author Contribution

*The authors confirm contribution to the paper as follows: **study conception and design:** Siti Noraiza Ab Razak, Ganesan Krishnan; **data collection:** Siti Noraiza Ab Razak, Ganesan Krishnan; **analysis and interpretation of results:** Mohamad Aizat Abu Bakar, Mundzir Abdullah; **draft manuscript preparation: :** Siti Noraiza Ab Razak, Nurul Nadia Adnan, Muhammad Sufi Roslan, Nik Noor Haryatul Eleena Nik Mahmud. All authors reviewed the results and approved the final version of the manuscript.*

Funding

This research is sponsored by the organization.

References

[1] Al-Hamdani, Uhood J., Qusay M.A. Hassan, Ahmed M. Zaidan, H.A. Sultan, Kawkab Ali Hussain, C.A. Emshary, and Zainab T.Y. Alabdullah (2022) Optical Nonlinear Properties and All Optical Switching in a Synthesized Liquid Crystal, *Journal of Molecular Liquids,* 361(5), 119676. https://doi.org/10.1016/j.molliq.2022.119676

[2] Durak, S., and S. Sakiroglu (2023) Theoretical Investigation of Laser Field Effect on Nonlinear Optical Properties of Quantum Dots, *Physica B: Condensed Matter,* 650, 414575. https://doi.org/10.1016/j.physb.2022.414575

[3] Wu, J.; Li, Z.; Luo, J.; Jen, K.Y. (2022) High-performance organic second- and third-order nonlinear optical materials for ultrafast information processing, *Journal of Materials Chemistry,* 8(43), 15009–15026. https://doi.org/10.1039/d0tc03224g

[4] B. Chen, D. Fang, L. Chen, X. Shen, J. Wei, D. Wang, and X. Chen (2023) Adjusting the nonlinear optical and optical limiting properties of MAPbBr3/PMMA by doping with Zn, *Materials Chemistry and Physics,* 309, 128310 https://doi.org/10.1016/j.matchemphys.2023.128310

[5] A. Suresh, N. Manikandan, R. M. Jauhar, P. Murugakoothan, and G. Vinitha (2018) Growth and characterization of urea p-nitrophenol crystal: an organic nonlinear optical material for optoelectronic device application, *Applied Physics A,* 124(6), 1-10. https://doi.org/10.1007/s00339-018-1767-2

[6] R. W. Boyd, A. L. Gaeta, and E. Giese (2008) *Nonlinear Optics. 3rd ed. Springer Handbook of Atomic,* Molecular and Optical Physics. https://link.springer.com/chapter/10.1007/978-3-030-73893-8_76

[7] C. Gayathri, and A. Ramalingam (2008) Investigation of optical nonlinearities of an azo dye using a 532 nm diode-pumped Nd: YAG laser, Spectrochimica Acta Part A: *Molecular and Biomolecular Spectroscopy*, 69(1), 96-99 https://doi.org/10.1016/j.saa.2007.03.025

[8] U. J. Al-Hamdani, Q. M. Hassan, M. J. Mohammed, H. A. Sultan, A. M. Dhumad, C. A. Emshary, and R. A. Alharis (2023) Synthesis and investigation of nonlinear optical properties of Azo-SR8 compound using visible laser beams, *Optical Materials*, 143, 114293 https://doi.org/10.1016/j.optmat.2023.114293

[9] M. Jamali, S. Mohajer, S. Sheikhlary, and M. H. M. Ara, M. H. M (2022) Z-scan optical method complements the Thioflavin T assay for investigation of anti-Alzheimer's impact of polyphenols, *Photodiagnosis and Photodynamic Therapy*, 39, 102914 https://doi.org/10.1016/j.pdpdt.2022.102914

[10] R. S. S. Kumar, S. V. Rao, L. Giribabu, and D. N. Rao (2009) Ultrafast nonlinear optical properties of alkyl phthalocyanines investigated using degenerate four-wave mixing technique, *Optical Materials,* 31(6), 1042-1047 https://doi.org/10.1016/j.optmat.2008.11.018

[11] A. J. Kiran, D. Udayakumar, K. Chandrasekharan, A. V. Adhikari, and H. D. Shashikala (2006) Z-scan and degenerate four wave mixing studies on newly synthesized copolymers containing alternating substituted

thiophene and 1, 3, 4-oxadiazole units, *Journal of Physics B: Atomic, Molecular and Optical Physics*, 39(18), 3747 https://doi.org/10.1088/0953-4075/39/18/005

[12] M. Moran, C. Y. She, and R. Carman (1975) Interferometric measurements of the nonlinear refractive index coefficient relative to CS 2 in laser-system-related materials, *IEEE Journal of Quantum Electronics,* 11(6), 259-263. https://doi.org/10.1109/JQE.1975.1068611

[13] R. Adair, L. L. Chase, and S. A. Payne (1987) Nonlinear refractive-index measurements of glasses using three-wave frequency mixing, *Journal of the Optical Society of America B,* 4(6), 875-881. https://doi.org/10.1364/JOSAB.4.000875

[14] E. W. Van Stryland, and M. Sheik-Bahae (1997) *Z-scan technique for nonlinear materials characterization. Materials characterization and optical probe techniques: a critical review*, SPIE:Vol. 10291, pp. 488-511. https://doi.org/10.1117/12.279853

[15] M. Yin, H. P. Li, S. H. Tang, and W. Ji (2000) Determination of nonlinear absorption and refraction by single Z-scan method, *Applied Physics B,* 70, 587-591. https://doi.org/10.1007/s003400050866

[16] K. Mani Rahulan, G. Vinitha, S. Ganesan, R. Philip, and P. Aruna, P (2012) Synthesis and optical limiting studies of HA P and HA P@ SiO 2 core–shell nanoparticles, *Journal of Materials Science: Materials in Electronics,* 23, 877-881. https://doi.org/10.1007/s10854-011-0510-y

[17] M. Sheik-Bahae, A. A. Said, T. H. Wei, D. J. Hagan, and E. W. Van Stryland (1990) Sensitive measurement of optical nonlinearities using a single beam, *IEEE journal of quantum electronics*, 26(4), 60-769. https://doi.org/10.1109/3.53394

[18] M. H. Anandalli, R. F. Bhajantri, S. R. Maidur, L. A. Shastri, and V. Sasirekha (2023) Dominant role of organic dye on Mn: ZnS/PMMA polymer nanocomposites: Structural, thermal, linear, and nonlinear optical properties for optoelectronic and photonic applications, *Materials Today Communications,* 35, 105918 https://doi.org/10.1016/j.mtcomm.2023.105918

[19] P. Gong, F. Liang, L. Kang, X. Chen, J. Qin, Y. Wu, and Z. Lin (2019) Recent advances and future perspectives on infrared nonlinear optical metal halides, *Coordination Chemistry Reviews,* 380, 83-102 https://doi.org/10.1016/j.ccr.2018.09.011

[20] S. Mirershadi, S. Ahmadi-Kandjani, A. Zawadzka, H. Rouhbakhsh, and B. Sahraoui (2016) Third order nonlinear optical properties of organometal halide perovskite by means of the Z-scan technique, *Chemical Physics Letters,* 647, 7-13. https://doi.org/10.1016/j.cplett.2016.01.041

[21] L. Zhou, H. Fu, T. Lv, C. Wang, H. Gao, D. Li, and W. Xiong (2020) Nonlinear optical characterization of 2D materials, *Nanomaterials*, 10(11), 2263. https://doi.org/10.3390/nano10112263

[22] S. O. Giwa, L. A. Chuah, and N. M. Adam (2014) Fuel properties and rheological behavior of biodiesel from egusi (Colocynthis citrullus L.) seed kernel oil, *Fuel Processing Technology*, 122, 42-48. https://doi.org/10.1016/j.fuproc.2014.01.014

[23] M. Ventura, E. Simionatto, L. H. C. Andrade, E. L. Simionatto, D. Riva, and S. M. Lima (2013): The use of thermal lens spectroscopy to assess oil–biodiesel blends, *Fuel*, 103, 506-511. https://doi.org/10.1016/j.fuel.2012.08.027

[24] F. Z. Zahadi, S. S. Yahya, and S. N. Ab Razak (2022) Conversion of Waste Cooking Oil into Biodiesel, *Multidisciplinary Applied Research and Innovation,* 3(5), 36-42. https://publisher.uthm.edu.my/periodicals/index.php/mari/article/view/8690

[25] J. Pelemo, K. T. Akindeji, F. L. Inambao, O. Awogbemi, and E. I. Onuh, (2022) A Comparative Evaluation of Biodiesel and Used Cooking Oil as Feedstock for HDRD Application: A Review, *Diesel Engines and Biodiesel Engines Technologies*, 61. https://doi.org/10.5772/intechopen.104393

[26] C. R. Parra, A. Corrêa-Guimarães, L. M. Navas-Gracia, C. R. A. Narváez D. Rivadeneira, D. Rodríguez, and A. D. Ramirez (2022) Bioenergy on islands: an environmental comparison of continental palm oil vs. local waste cooking oil for electricity generation, *Applied Sciences* 10(11), 3806. https://doi.org/10.3390/app10113806

[27] M. A. H. Lokman NolHakim, N. A. M. Shohaimi, W. N. A. W. Mokhtar,M. L. Ibrahim, and R. F. Abdullah (2011) Immobilization of potassium-based heterogeneous catalyst over alumina beads and powder support in the transesterification of waste cooking oil, *Catalysts,* 11(8), 976. https://doi.org/10.3390/catal11080976

[28] R. Abd Rabu, I. Janajreh, and D. Honnery (2013) Transesterification of waste cooking oil: Process optimization and conversion rate evaluation, *Energy Conversion and Managemen,t* 65, 764-769 https://doi.org/10.1016/j.enconman.2012.02.031

[29] H. L. MacLean, L. B. Lave, R. Lankey, and S. Joshi (2000) A life-cycle comparison of alternative automobile fuels, *Journal of the air & waste management association*, 50(10), 1769-1779. https://doi.org/10.1080/10473289.2000.10464209

[30] N. Mansir, S. H. Teo, U. Rashid, M. I. Saiman, Y. P. Tan, G. A. Alsultan, and Y. H. Taufiq-Yap (2018) Modified waste egg shell derived bifunctional catalyst for biodiesel production from high FFA waste cooking oil. A review, *Renewable and Sustainable Energy Reviews,* 82, 3645-3655. https://doi.org/10.1016/j.rser.2017.10.098

[31] O. A. Falowo, B. Oladipo, A. E. Taiwo, A. T. Olaiya, O. O. Oyekola, and E. Betiku (2022) Green heterogeneous base catalyst from ripe and unripe plantain peels mixture for the transesterification of waste cooking oil, *Chemical Engineering Journal Advances,* 10, 100293. https://doi.org/10.1016/j.ceja.2022.100293

[32] M. M. Ali, S. M. Ahmed, D. Y. Aqar, S. A. Gheni, G. H. Abdullah, M. A. Mahmood, and A. N. Phan (2022) Use of dolomite catalyst in biodiesel production via transesterification of waste cooking oil in oscillatory baffled reactor, *AIChE Journal*, 68(9), e17751. https://doi.org/10.1002/aic.17751

[33] N. A. A. Shah, F. N. Diauddin, S. Z. N. Demon, N. Kasim, G. Krishnan, and M. Abdullah (2022) Preparation and third order nonlinear optical properties of Ag coated carbon nanotubes, *Materials Today: Proceedings*, 29, 110-114. https://doi.org/10.1016/j.matpr.2020.05.680

[34] I. Dancus, I., A. Petris, P. Doia, E. Fazio, and V. I. Vlad, *Z-Scan measurement of thermal optical nonlinearities. In ROMOPTO 2006: Eighth Conference on Optics*, 2007;SPIE:Vol. 6785, pp. 380-385. https://doi.org/10.1117/12.757946

[35] R. De Nalda, R. Del Coso, J. Requejo-Isidro, J. Olivares, A. Suarez-Garcia, J. Solis, J., and C. N. Afonso (2002) Limits to the determination of the nonlinear refractive index by the Z-scan method, *Journal of the Optical Society of America B,* 19(2), 289-296. https://doi.org/10.1364/JOSAB.19.000289

[36] A. Krishnasamy, and K. R. Bukkarapu (2021) A comprehensive review of biodiesel property prediction models for combustion modeling studies, *Fuel,* 302, 121085. https://doi.org/10.1016/j.fuel.2021.121085

[37] M. M. Roy, W. Wang, and J. Bujold (2013) Biodiesel production and comparison of emissions of a DI diesel engine fueled by biodiesel–diesel and canola oil–diesel blends at high idling operations, *Applied Energy*, 106, 198-208. https://doi.org/10.1016/j.apenergy.2013.01.057

[38] F. L. S. A. Cuppo, A. M. F. Neto, S. L. Gómez, and P. Palffy-Muhoray (2002) Thermal-lens model compared with the Sheik-Bahae formalism in interpreting Z-scan experiments on lyotropic liquid crystals, *Journal of the Optical Society of America B*, 19(6), 1342-1348. https://doi.org/10.1364/JOSAB.19.001342

[39] T. Geethakrishnan, and P. K. Palanisamy (2007) Z-scan determination of the third-order optical nonlinearity of a triphenylmethane dye using 633 nm He–Ne laser, *Optics Communications,* 270(2), 424-428. https://doi.org/10.1016/j.optcom.2006.09.035

[40] M. I. Rosli, A. Awalludin, M. Duralim, M. Abdullah, and M. S. Abd Aziz (2020) Study on The Third Order NLO Properties of Trace Metal Ions in Nitric Acid Solution by Closed-Aperture Z-scan Technique, *Journal of Physics: Conference Series,* 1484(1), 012005. https://doi.org/10.1088/1742-6596/1484/1/012005

[41] M. I. Rosli, M. Abdullah, G. Krishnan, S. W. Harun, and M. S. Aziz (2020) Power-dependent nonlinear optical behaviours of ponceau BS chromophore at 532 nm via Z-scan technique, *Journal of Photochemistry and Photobiology A: Chemistry,* 397, 112574. https://doi.org/10.1016/j.jphotochem.2020.112574

[42] M. Sheik-Bahae, A. A. Said, T. H. Wei, Y. Y. Wu, D. J. Hagan, M. J., Soileau, and E. W. Van Stryland (1990) Z-scan: a simple and sensitive technique for nonlinear refraction measurements, *Nonlinear Optical Properties Of Materials,* 1178, 41-51. https://doi.org/10.1117/12.962142